

# NOVEL X-RAY BEAM POSITION MONITOR FOR COHERENT SOFT X-RAY BEAMLINES\*

B. Podobedov<sup>1,†</sup>, D.M. Bacescu<sup>1</sup>, D. Donetski<sup>2</sup>, C. Eng<sup>1</sup>, S.L. Hulbert<sup>1</sup>, K. Kucharczyk<sup>2</sup>, J. Liu<sup>2</sup>,  
 R. Lutchman<sup>2</sup>, C. Mazzoli<sup>1</sup>, C.S. Nelson<sup>1</sup>, J. Zhao<sup>2</sup>

<sup>1</sup>Brookhaven National Laboratory, Upton, NY, USA

<sup>2</sup>Stony Brook University, Stony Brook, NY, USA

## Abstract

A novel soft X-ray BPM (sXBPM) for high-power white beams of synchrotron undulator radiation is being developed through a joint effort of BNL/NSLS-II and Stony Brook University. In our approach, custom-made multi-pixel GaAs detector arrays are placed into the outer portions of the X-ray beam, and the beam position is inferred from the pixel photocurrents. Our goal is to achieve micron-scale positional resolution  $\sim 30$   $\mu$ m away from the source, without interfering with user experiments, especially the most sensitive ones exploiting coherent properties of the beam. To this end, an elaborate mechanical system has been designed, fabricated, and installed in the 23-ID canted undulator beamline first optical enclosure (FOE), which allows positioning of the detectors with micron-scale accuracy, and provisions for possible intercepts of kW-level beam in abnormal conditions. Separately, GaAs detectors with specially tailored spectral response have been designed, fabricated, and tested in the soft and hard X-ray regions at two NSLS-II beamlines. This paper gives an overview of the sXBPM system and presents the first preliminary results from the high-power white X-ray beam.

## INTRODUCTION

Non-invasive soft X-ray BPMs (sXBPMs) do not exist yet but are greatly desired for coherent soft X-ray beamlines. We are working to develop such sXBPM for high-power, white X-ray beams. In our approach [1], multi-pixel GaAs detector arrays are placed into the outer portions of X-ray beam, away from the undulator central cone. Beam position, together with other information, is inferred from the pixel photocurrents, see Fig. 1.

Potential advantages of this approach include much higher sensitivity of GaAs compared to metal blades used in conventional photoemission type XBPM designs for hard X-rays [2, 3]. Also, with pixelated detectors, we expect better positional resolution, spatial feature resolution, smaller systematic errors due to undulator gap changes (and phase changes for EPUs), and the ability to discriminate stray light from bending magnets and other sources. The last two are long-standing challenges for the conventional hard X-ray XBPMs (e.g., [4]).

The main challenges with our approach are that the device must have adequate responsivity in soft X-ray; it must withstand high power, potentially leading to elevated diode junction temperature and high pixel photocurrents, and it must reliably operate in UHV.

The first goal of our R&D program to investigate this approach includes the design, fabrication, and demonstration of suitable performance of the detector arrays. The second goal is to design, fabricate, and install the sXBPM into the 23-ID FOE, where movable sXBPM detectors intercept the outer portions of white X-ray beam (Fig. 1) from two identical APPLE-II undulators (EPU49,  $L=2$  m each, 2.5 m center-to-center spacing), nominally canted at 0.16 mrad. Each undulator serves as a primary radiation source for one of the two soft X-ray beamlines, CSX or IOS. Our final goal is to demonstrate micron-scale positional resolution of the sXBPM at the sampling rate of 10 Hz or higher for the undulator fundamental harmonic ( $E_1$ ) tuned in the range of  $E_1=250-2000$  eV covering the operating energy range of the beamlines.

Figure 1 shows the maximum expected power density at the sXBPM location from a single (downstream) undulator tuned to  $K=3.458$  ( $E_1=250$  eV) in linear horizontal polarization. Due to the FOE mask (fixed water-cooled aperture)  $\sim 1$  m upstream of the sXBPM, the photons outside a  $\sim 5 \times 10$  mm<sup>2</sup> rectangle (shown in dash) are not accessible for detection. During user operations, the beam from the other undulator, independently tuned in the range of  $E_1=250-2000$  eV, is also present. In this (canted) configuration the two beams are displaced horizontally at the sXBPM location by about  $\pm 2$  mm with respect to the center of the mask. The photon beam can be further clipped by front-end (FE) slits, located in the ring tunnel  $\sim 7$  m upstream of the sXBPM.

To install the sXBPM into an operating beamline our design must guarantee no interference with beamline operations under all possible scenarios. Therefore, the detectors are placed on movable blades, which can be completely removed (parked in the FOE mask shade) or positioned to intercept any desired fraction of the beam.

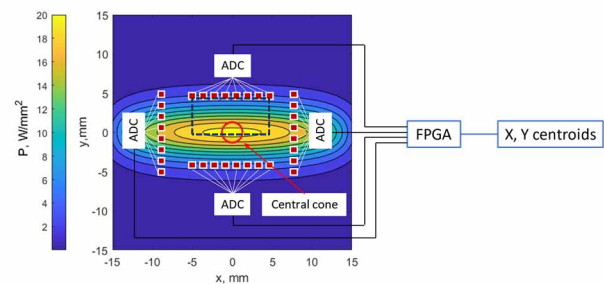


Figure 1: sXBPM concept (detector pixels shown overlaid on the X-ray power density distribution 26 m away from a single EPU in the non-canted configuration).

<sup>†</sup> boris@bnl.gov

## DETECTOR DEVELOPMENT

Details about detector development, fabrication, and testing can be found in Ref. [5]. Briefly, GaAs was selected due to mature material growth and processing technology, ability to operate at high current densities and elevated temperatures. Wafers were grown by solid-source Molecular Beam Epitaxy for the highest material quality and doping control. For studies, photodiode arrays with up to 64 pixels were fabricated with rectangular pixel sizes from  $2 \times 6$  to  $60 \times 50 \mu\text{m}^2$ ; round pixels were used in later designs (Fig. 2).

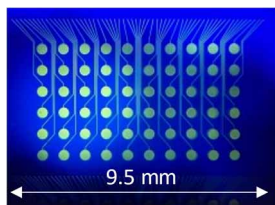


Figure 2: Diode array with contact pads before cleaving.

The sXBPM detectors must have spectral coverage (high responsivity) from  $\sim 650$  eV to at least 2 keV, as defined by low-K undulator operation, where the intercepted power density is relatively small. At high K, high power is mainly coming from hard X-rays, even for the pixels positioned far away from the beam center (see figures in the accompanying talk). This regime requires low hard X-ray responsivity to maintain manageable photocurrent density levels. Such spectral response of the detector was accomplished by shallow p-n junction design.

The responsivity was measured with a high-power Ar-Ion laser in the visible range, as well as in two NSLS-II beamlines, one soft X-ray (23-ID-1, CSX) and one hard X-ray (4-ID, ISR). The required spectral response was confirmed.

Figure 2 shows one of the fabricated arrays targeted for white-beam installation: 60 mesa photodiodes with a  $16\text{-}\mu\text{m}$  mesa diameter isolated by silicon nitride with  $8\text{-}\mu\text{m}$  windows for the top metallization connecting the pixels of the linear array to 6 rows of  $400\text{-}\mu\text{m}$  diameter contact pads. The distance from the mesa photodiode to the cleaved edge of the array was about  $20 \mu\text{m}$ . The array length of  $\sim 1$  cm matches the FE mask opening at the sXBPM location. The pixel spacing of  $160 \mu\text{m}$  should allow one to resolve the expected shapes of the X-ray beam. Temporal variation of pixel photocurrents will be used to extract the beam centroid position vs. time.

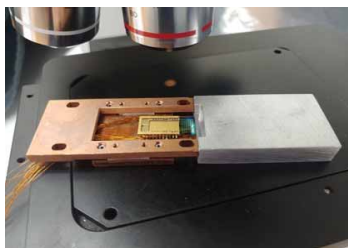


Figure 3: Detector assembly pre-alignment.

Special attention was given to the packaging of the detectors for the UHV operation. To bring the detected signals out-of-vacuum we went with individual Kapton-coated  $120 \mu\text{m}$  diameter copper wires routed to the UHV feedthrough. Our first design assumed direct soldering to the contact pads, which turned out to be challenging due to tight space. We ended up wire-bonding the pixels to gold-plated pads of a ceramic carrier with wire leads (Fig. 3). The next design iteration had a ceramic interposer with two rows of gold-plated pads for wire bonds and three rows of pads for soldering wires.

The detectors operate in the photovoltaic mode (no DC bias) with transimpedance amplifiers for I-V conversion and 24-bit ADC USB5801 modules from Advantech are used for the data acquisition. Time domain multiplexing of the I-V converters is being added for the upcoming installation.

## SXBPM DESIGN AND INSTALLATION

Mechanical design details can be found in Ref. [6]. The design had to address several unique challenges, including: 1) micron-level stability of the assembly, 2) management of the heat load from undulator X-ray beams (each EPU can radiate upwards of 3 kW), 3) assembly compactness to fit within the existing FOE, and 4) accessibility for modifications. All installations had to be carefully planned for machine shutdowns to not interfere with the user operations of the two 23-ID beamlines.

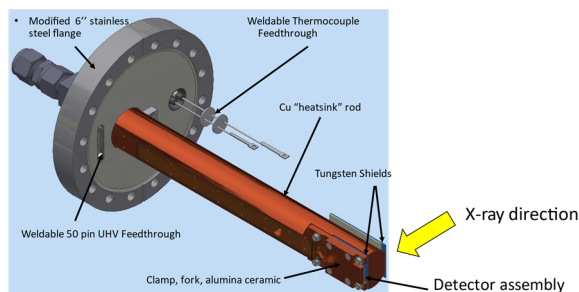


Figure 4: sXBPM blade assembly.

The sXBPM contains up to four water-cooled blade assemblies (Fig. 4), with their flanges mounted on bellows-coupled stepper-motor-driven linear manipulators, so that the blades can be inserted into the X-ray beam with sub-micron accuracy and resolution. Each blade assembly has a GaAs detector array mounted at the tip of the blade and aligned with respect to the tungsten shields upfront, such that only about a  $50 \mu\text{m}$ -high area of the photodiode array is intercepting the X-ray beam. This limits the maximum heat power dissipation in the array itself to about 10 W, which is acceptable according to our thermal modeling.

The sXBPM 6-way cross is mounted on a high-stability Invar stand and is bracketed by two vacuum isolation valves. So far, only the top blade assembly with the detectors was installed and tested. A photo of the sXBPM as installed in 23-ID FOE is shown in Fig. 5.

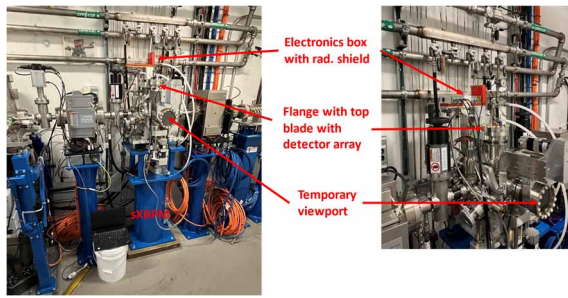


Figure 5: sXBPM installed in 23-ID FOE.

## FIRST RESULTS

The top sXBPM blade equipped with a detector array was installed in May 2023. Only 4 array pixels were connected to the data acquisition electronics outside. After the installation, we were limited by the vacuum conditions, so, during user operations, the detector had to be parked in the shade of the FOE mask. However, during low-current machine studies, we were able to bring the detector out of the shade and scan it across the entire X-ray beam while varying the EPU gaps.

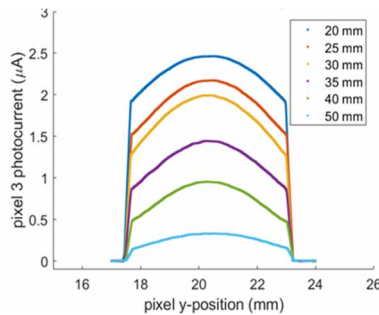


Figure 6: Vertical scans at different EPU2 gaps;  $I= 2$  mA.

Figure 6 shows the photocurrent from one of the pixels recorded during these scans, when the upstream EPU gap was fully open, and the gap of the downstream EPU (EPU2) was varied in the [20-50] mm range, corresponding to the K parameter values of [2.6-0.4]. The 5-mm clipped width of all curves is due to the FOE mask vertical opening. Inside the opening, the signals traced the expected X-ray beam shapes, decreasing in intensity and narrowing with larger ID gaps. Importantly, no noise or parasitic signals were observed when the detector was positioned outside the FOE mask aperture.

Additional tests included closing the vertical FE slits and observing, as expected, further reduction of the intercepted beam height, as well as the observation of diffraction lobes near the projected edges of the slits (see talk).

As the sXBPM vacuum conditioning progressed, during high-current user operations we were able to bring the detector very close to the edge of the projected slits, so that the pixels were partially illuminated with diffracted X-rays. Even in these sub-optimal conditions, the pixel signals were clearly registering top-off injection transients, as well as tracking the EPU gap changes (see talk), which change the X-ray beam shape and intensity at the sXBPM detector location.

During the final days before the August 2023 machine shutdown the improved vacuum conditions have finally allowed us to bring the detector completely out of the shade. During user operations at 500 mA, the pixel signals were reading (depending on the EPU gap settings) up to  $\sim 120$   $\mu\text{A}$  with fairly low noise. They were changing, as expected, in response to the topoff injections, small orbit motions, EPU gap changes, etc. We are still performing a detailed comparison of the recorded data against the synchrotron radiation modeling which will be presented separately.

Figure 7 shows the signal from one of the pixels while the detector was extracted vertically upwards, in 50  $\mu\text{m}$  steps, from the initial position  $\sim 1.4$  mm away from the beam center. The signals were recorded at the sampling rate of 6 kS/s, and then each group of 512 samples was averaged, so the plotted sampling rate is  $\sim 12$  Hz.

The 50- $\mu\text{m}$  steps result in the corresponding step-wise reduction of the signal intensity seen in Fig. 7 as the detector moved vertically away from the X-ray beam center.

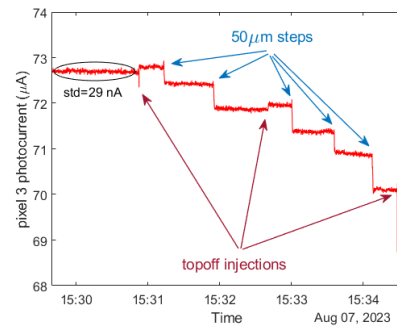


Figure 7: Pixel photocurrent during stepped extraction of the detector;  $I=500$  mA, EPU2 gap at 30 mm.

Between the steps, the signal standard deviation is  $\sim 30$  nA. Dividing this number by the current steps resulting from stepping the detector, measuring 0.35 to 0.74  $\mu\text{A}$  in Fig. 7, we get that, depending on the detector location, the measured signal standard deviation is equivalent to a pixel rms motion ranging from 2 to 4 microns. These measurements give us a crude upper-bound estimate of the achievable positional resolution of the sXBPM. Based on these results, we are confident in meeting or exceeding our goal of micron-scale sXBPM resolution in the future, when we use symmetrically positioned arrays, multi-pixel X-ray beam position calculation algorithms, and optimized electronics.

## CONCLUSION

Our R&D program investigates a novel approach to white-beam XBPMs targeting coherent soft X-ray synchrotron beamlines, where no other viable solutions exist.

To date, the required GaAs detectors have been designed, fabricated, and tested. Their responsivity from sub-keV to a few keV photon energies was accomplished with shallow p-on-n junction design. Detector arrays have been extensively characterized with a high-power Ar-ion laser, and then tested in a monochromatic beam at soft- and hard X-ray beamlines of NSLS-II. The sXBPM prototype with

a single detector array assembly was recently installed in the high-power X-ray white beam from two canted EPUs in the C23-ID straight. The device successfully resolved small beam and detector motions and gap-change-induced variations of X-ray beam shape during 500 mA user operations. To the best of our knowledge, this is the first successful attempt to use multi-pixel semiconductor detectors as diagnostics for high-power white-beam undulator radiation.

Our immediate future steps include the installation of a symmetric top-bottom sXBPM configuration with 25 wired pixels per blade and with optimized electronics. Studies of achievable X-ray beam position resolution and other XBPM performance metrics, as well as the optimization of beam position algorithms tailored to multi-pixel detectors, will follow.

Our longer-term plans include the investigation of sXBPMs with fixed-position detectors or with detectors combined with (adjustable) primary slits. Another promising direction includes analog-to-digital conversion performed in UHV immediately adjacent to the detector followed by a serial communication to the electronics outside, which should significantly reduce the number of signal wires needed to be brought out from the UHV volume. All of these potential upgrades are expected to reduce the cost of the device. Investigating designs tailored for hard X-ray beamlines is also an option.

We believe our innovative approach holds significant promise for enhancing synchrotron beamline and accelerator diagnostics, especially for highly coherent beams in future diffraction-limited light sources.

## ACKNOWLEDGEMENTS

Our project is supported by the U.S. Department of Energy, Office of Science, Office of Basic Energy Sciences, Accelerator & Detector Research Program of Scientific User Facilities Division. This research used beamlines 4-ID (ISR), 23-ID-1 (CSX), and 23-ID-2 (IOS) of the NSLS-II, a DOE Office of Science User Facility operated for the DOE Office of Science by Brookhaven National Laboratory under Contract No. DE-SC0012704.

## REFERENCES

- [1] J. Liu *et al.*, “Progress towards soft x-ray beam position monitor development”, in *Proc. IPAC'21*, Campinas, Brazil, May 2021, pp. 438-441.  
doi:10.18429/JACoW-IPAC2021-MOPAB121
- [2] E. D. Johnson and T. Oversluizen, “Compact high flux photon beam position monitor”, *Rev. Sci. Instrum.*, vol. 60, no. 7, pp. 1947-1950, 1989. doi:10.1063/1.1140896
- [3] D. Shu, B. Rodricks, J. Barraza, T. Sanchez, and T. M. Kuzay, “The APS X-ray undulator photon beam position monitor and tests at CHESS and NSLS”, *Nucl. Instrum. Methods Phys. Res., Sect. A*, vol. 319, nos. 1-3, pp. 56-62, 1992.  
doi:10.1016/0168-9002(92)90531-8
- [4] G. Decker and O. Singh, “Method for reducing x-ray background signals from insertion device x-ray beam position monitors”, *Phys. Rev. Accel. Beams*, vol. 2, no. 11, p. 112801, 1999.  
doi:10.1103/PhysRevSTAB.2.112801
- [5] D. Donetski *et al.*, “High power density soft x-ray GaA photodiodes with tailored spectral response”, *Semicond. Sci. Technol.*, vol. 37, p. 085024, 2022.  
doi:10.1088/1361-6641/ac7c88
- [6] C. Eng, D. Donetski, J. Liu, S. Hulbert, C. Mazzoli, and B. Podobedov, “Mechanical design of a soft x-ray beam position monitor for the coherent soft x-ray scattering beamline”, in *Proc. MEDSI'20*, Chicago, USA, Jul. 2021, pp. 56-58. doi:10.18429/JACoW-MEDSI2020-MOPC01